Optical Vector Network Analyzer with an Improved Dynamic Range Based on a Polarization Multiplexing Electro-Optic Modulator *

Qi Wang(王琪)[1,2], Wen-Ting Wang(王文亭)[1,2**], Wei Chen(陈伟)[1], Jian-Guo Liu(刘建国)[1], Ning-Hua Zhu(祝宁华)[1]

[1]*Laboratory of Solid State Optoelectronic Information Technology, Institute of Semiconductors, Chinese Academy of Sciences, Beijing 100083*

[2]*College of Materials Science and Opto-Electronic Technology, University of Chinese Academy of Sciences, Beijing 100049*

(Received 4 November 2016)

We present a new method to achieve an optical vector network analyzer (OVNA) based on a polarization multiplexing electro-optic modulator (PM-EOM) without an optical bandpass filter. Optical single sideband (OSSB) modulated signals with a tunable optical carrier-sideband ratio (OCSR) are obtained at the output of the PM-EOM. The OCSR can be flexibly tuned by controlling bias voltages of the PM-EOM. The dynamic range of the OVNA is expanded by taking the improvement of the OCSR into account. The transmission response of an optical device under test (ODUT) is measured based on one-to-one mapping from optical domain to electrical domain. By optimizing the OCSR of the OSSB modulated signals, the dynamic range of the OVNA can be effectively improved with 3.7 dB. An analytical model is derived to describe the transfer function of the ODUT. The magnitude and phase responses of a fiber Bragg grating are characterized with a large dynamic range.

PACS: 42.79.Hp, 42.79.Sz, 42.30.Lr, 42.60.Fc, 42.25.Ja DOI: 10.1088/0256-307X/34/5/054205

High precision characterization for magnitude and phase responses of optical components or optical links is really important in the advanced photonic integrated circuits (PIC) and optical device fabrication. The optical vector network analyzer (OVNA) has been emerging as a promising method to accurately measure the transmission responses of optical devices or links.[1] Conventional measurement methods are based on phase-shift modulation,[2] and interferometric methods[3] have been available. However, in both the approaches, the measurement resolution is limited to 1 pm by the wavelength tunning resolution of wavelength-swept laser sources. For some ultrahigh-Q optical devices, the resolution is unable to characterize the response effectively. The magnitude and phase features inside the resolution range cannot be correctly displayed.

Alternatively, the OVNA based on optical single sideband (OSSB) modulation has no such restriction. In the past decade, there have been numerous methods to achieve OSSB modulation by removing one of the sidebands of optical double sideband (ODSB) modulation. In these methods, a tunable optical bandpass filter (OBPF) with highly steep edges,[4] or a fiber Bragg grating,[5] is used. However, it is expected that the OVNA can work without optical wavelength dependence. The OSSB modulation can be achieved using a dual-drive Mach–Zehnder modulator (DMZM) with a 90 hybrid coupler which has a wide bandwidth and highly stability[6] or stimulated Brillouin scattering in a fiber.[7] Both magnitude and phase responses of an optical device under test (ODUT) are measured by one-of-one mapping by scanning the modulated sideband with a frequency tunning resolution as high as the Hz-level.[5] This kind of OVNA benefits from the maturing electrical techniques. It is more desirable for an OVNA to have higher resolution, better accuracy, and larger dynamic range, even though considerable progress has been made. The measurement error is especially worth considering for the OVNA, which generally derives from the beating between higher-order sidebands and residually unwanted first-order sidebands. Some studies have already demonstrated that the power ratio between the desired and undesired sidebands with 10 dB can introduce magnitude measurement errors by about 3 dB.[8] To suppress the measurement error, the driving microwave power should be limited to meet small signal modulation, which will in turn create a large optical carrier-sideband ratio (OCSR). It is still not good enough to eliminate the measurement errors completely although this method has already been working very well. Some methods have been reported to completely remove the measurement errors in the OVNA based on unbalanced ODSB modulation,[9] vector subtracting,[10] SBS in a highly nonlinear fiber (HNLF),[11] and dual-parallel Mach–Zehnder modulator (DPMZM).[12] A high spectral measurement accuracy is achieved. In addition to the

*Supported by the National Natural Science Foundation of China under Grant Nos 61377070, 61090391 and 61675196, and the National High-Technology Research and Development Program of China under Grant No 2013AA014203.

**Corresponding author. Email: wtwang13@semi.ac.cn

© 2017 Chinese Physical Society and IOP Publishing Ltd

resolution and measurement errors, improvement of the dynamic range of the OVNA is also important, especially for an ODUT with a pretty deep notch. For the OSSB-based OVNA, the desired first-order sideband of the OSSB modulated signal goes through the ODUT to monitor its magnitude and phase response. The weak first-order sideband will disappear close to the notch center, which restricts the dynamic range due to limited sensitivity of a photodetector (PD). Moreover, the optical carrier power cannot be infinitely amplified to avoid power saturation of the PD or gain saturation from an optical amplifier. In Ref. [9], the optical signal with different sideband suppression ratios (SSR) is used to measure an ODUT with two different measurements. Then, two equations need to be solved to obtain spectral responses of the OVNA. This method can expand the dynamic range of the measurement system, but it is complicated and may introduce some extra errors with two different measurements. Xue *et al.* proposed a powerful method to realize an OVNA based on a Hilbert transformer and a balanced photodetector to remove measurement errors and to improve measured dynamic range by adjusting SSR.[13] The two methods mentioned above improve the measured dynamic range of an OVNA in the same way in which the SSR is changed. However, the average input power for the PD will be changed when the SSR is adjusted. For some cases, the PD input power is limited by its maximum input power which will damage it. Therefore, it is more desirable to further enhance OVNA dynamic range under the maximum input optical power for a PD. An OVNA with improved dynamic range can be used for especially high-Q optical devices or systems, such as micro-resonator, phase-shifted Bragg grating, and SBS-based gain or loss spectra.

In this Letter, we propose a new approach to achieve OSSB-based OVNA using a PM-EOM without an OBPF. The dynamic range of the OVNA is improved by tuning the OCSR and keeping PD average input optical power constant. The OSSB modulated signal is generated at the PM-EOM output by properly adjusting its bias voltages and setting microwave signal power. The magnitude and phase of the OSSB signal is encoded by the transmission response of an ODUT, which is one-to-one mapped into the microwave domain by a PD. Both magnitude and phase responses of the ODUT are measured by sweeping the frequency of the microwave signal. The dynamic range of the OVNA is improved by 3.7 dB. The proposed approach is theoretically analyzed and experimentally demonstrated. The proposed method is wavelength-independent without an OBPF and has an improved dynamic range.

The schematic diagram of the proposed OVNA using a PM-EOM is shown in Fig. 1. An optical carrier at a frequency of $\omega_{\rm c}$ from a laser diode (LD) is fed into the PM-EOM via a polarization controller (PC1), which is used to align the polarization direction of the optical carrier so that it has a certain angle to the PM-EOM. The light wave is modulated by a microwave signal at a frequency of $\omega_{\rm m}$. The PM-EOM consists of two DPMZMs locating on two arms in parallel connected by a polarization beam splitter (PBS) and a polarization beam combiner (PBC). The OSSB modulated signals with a tunable OCSR are generated at the output of the PM-EOM. The optical carrier and the corresponding sideband are orthogonally polarized with each other. The optical signal is boosted by an erbium-doped optical fiber amplifier (EDFA) to keep the average optical power constant. The OSSB modulated signals are sent into an ODUT where the first-order sideband undergoes magnitude and phase modifications by the ODUT. The power variations of the optical sideband will be projected into the recovered microwave signal, which are recorded by an electrical vector network analyzer (EVNA). The inset of Fig. 1(a) shows the schematic diagram of the optical spectra after different optical devices to demonstrate the OSSB modulation. The electrical field at the input of PM-EOM is $\exp(j\omega_{\rm c}t)$. The microwave signal with $V_{\rm m}\cos(\omega_{\rm m}t+\varphi_{\rm m})$ is injected into the RF port of DPMZM1 to achieve optical frequency shifting,[14] where $V_{\rm m}$, $\omega_{\rm m}$ and $\varphi_{\rm m}$ are the amplitude, the angular frequency, and the initial phase of the RF signal, respectively. The DPMZM2 is not driven by a microwave signal to let the pure optical carrier pass through. The electrical field at the PM-EOM can be written as

$$\begin{aligned} E_x(t) &= \exp(j\omega_{\rm c}t)\cdot[\cos(\beta\cos(\omega_{\rm m}t+\phi_{\rm m}) \\ &\quad +\varphi_1/2)\exp(j\varphi_3)+\cos(\beta\cos(\omega_{\rm m}t \\ &\quad +\phi_{\rm m}+\pi/2)+\varphi_2/2)] \\ E_y(t) &= \cos\varphi_4\cos\varphi_5\cdot\exp(j\omega_{\rm c}t)\exp(j\varphi_6), \end{aligned} \quad (1)$$

where x and y show the two polarization directions of the PM-EOM, $\beta=\pi V_{\rm m}/V_\pi$, V_π is the half-wave voltage of MZMs, and $\phi_i=\pi V_{{\rm DC}_i}/V_{{\rm DC}_\pi}$ ($i=1$–6) is the phase shift controlled by the DC biases of the MZMs, with $V_{{\rm DC}_i}$ being the DC voltages of each MZM, and $V_{{\rm DC}_\pi}$ being the DC half-wave voltages. In our case, the MZMs locating in the DPMZM are biased at the minimum transmission points (MTP) to set $\phi_1=\phi_2=\pi$, $\phi_3=\pi/2$ and $\phi_6=0$ by adjusting the DC biases. The concept of SSB frequency shifting with a DPMZM was first presented.[15] The optical carrier is split into two parts and then injected into two MZM. Both MZMs are biased at MTP to suppress the optical carrier. The two MZMs are also driven by two microwave signals with 90° phase difference resulting in a destructive interference at the odd-order sidebands on either side of the optical carrier. Assuming $\varphi_{\rm m}=0$ and applying the Jacobi–Anger expan-

sion for Eq. (1), the electrical field at the PM-EOM output is

$$E_x(t) = 2J_1(\beta) \cdot \exp(j\omega_c t + j\omega_m t - j\pi/2),$$
$$E_y(t) = \cos\phi_4 \cdot \cos\phi_5 \cdot \exp(j\omega_c t), \quad (2)$$

where $J_n(\bullet)$ is the Bessel function of the first kind of order n. In this derivation, we make an assumption of small signal modulation so that $\beta \ll 1$ is required. Since the DPMZM is working under the frequency shifting condition, most of the power is lost leading to low conversion efficiency. The two optical signals are polarization multiplexed by the PBC. The polarized orthogonally OSSB signals are sent into the polarizer, which is used to project two polarization orthogonal components into a polarization direction. The electrical field at the output of the polarizer can be rewritten as

$$E_{out}(t) = 2J_1(\beta) \cdot \cos\theta \cdot \exp(j\omega_c t + j\omega_m t - j\pi/2) + \cos\phi_4 \cdot \cos\phi_5 \cdot \sin\theta \cdot \exp(j\omega_c t), \quad (3)$$

where θ is the angle between the principle axis of the PBC and the polarizer direction. We define the OCSR as the power ratio between the optical carrier and the corresponding first-order sideband, which can be expressed as OCSR=$10 \times \log_{10}(P_{1st}/P_{OC})$. The OSSB modulated signal passes through the ODUT to monitor its magnitude and phase responses. The corresponding output electrical field can be expressed as

$$E_{ODUT}(\omega) = E_{out}(\omega) \cdot H_{ODUT}(\omega)$$
$$= -A_1 \cdot \delta[\omega - (\omega_c + \omega_m)]H_{ODUT}(\omega_c + \omega_m) + A_0 \cdot \delta(\omega - \omega_c)H_{ODUT}(\omega_m), \quad (4)$$

where $A_1 = 4\pi j J1(\beta)\cos(\theta)$, $A_0 = 2\pi\cos(\phi_4)\cos(\phi_5)\sin(\theta)$, and $H_{ODUT}(\omega)$ and $E_{out}(\omega)$ are the transmission response of the ODUT and the Fourier transform of the output electrical field of PM-EOM, respectively. After square-law detection in the PD, the generated photocurrent is

$$i_{PD}(\omega) = \eta \cdot E_{ODUT}(\omega) \cdot E^*_{ODUT}(\omega), \quad (5)$$

where η is the responsivity of the PD. For a given PD, the responsivity is constant. EVNA can only respond to the signal it generates. Therefore, the photocurrent at the frequency of ω_m can be written as

$$i_{PD}(\omega_m) \propto A_0 A_1 H_{ODUT}(\omega_c + \omega_m)H^*_{ODUT}(\omega_m). \quad (6)$$

Therefore, the transmission response of the ODUT is

$$H_{ODUT}(\omega_c + \omega_m) = i_{PD}(\omega_m)/A_0 A_1 H^*_{ODUT}(\omega_m). \quad (7)$$

In general, a calibration process needs to be carried out to remove the inherent response of the whole system without the ODUT. We can define the transmission response of the OVNA system without the ODUT as $H_{I(\omega_c+\omega_m)}$. Therefore, the real transmission response of the ODUT can be expressed as $H(\omega_c + \omega_m) = H_{ODUT(\omega_c+\omega_m)}/H_{I(\omega_c+\omega_m)}$. As can be seen from Eq. (7), the measured dynamic range of the proposed OVNA can be expanded by improving system parameters. Keeping the average input optical power constant, the largest dynamic range can reach OCSR=0 dB. The optical carrier has an amplitude of A_0 and hence the corresponding optical power is $[A_0]^2$. The desired optical sideband power is $[A_1]^2$. Keeping the PD input optical average power constant, we can achieve the largest dynamic range when $A_0 = A_1$, because the recovered microwave signal varying with cross produce A_0A_1 is obtained by the beating between optical carrier and the optical sideband.[16] Compared with the methods in Refs. [8,13], the proposed method can further improve the dynamic range of an OVAN. Therefore, in our scheme, we firstly obtain the largest SSR to ensure the optimum dynamic range for this case and then we optimize the OCSR to further enhance it. It is worth noting that the dynamic range improvement by SSR is monotonic increasing but the dynamic range improvement by OCSR has an optimum point at OCSR=0 dB. Moreover, by improving the responsivity or increasing the maximum input optical power for the PD, the dynamic range can also be effectively expanded.

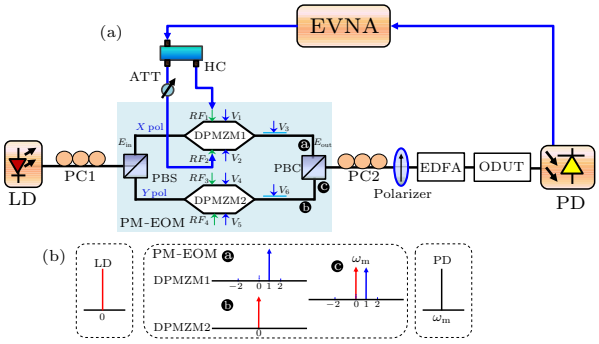

Fig. 1. Schematic diagram of the proposed scheme for the optical vector network analyzer with dynamic range improvement. LD: laser diode; PC1, PC2: polarization controller; PM-EOM: polarization multiplexing electro-optic modulator; PBS: polarization beam splitter; DPMZM: dual-parallel Mach–Zehnder modulator; PBC: polarization beam combiner; EDFA: erbium-doped fiber amplifier; ODUT: optical device-under-test; PD: photodetector; EVNA: electrical vector network analyzer, HC: hybrid coupler; and ATT: attenuator. Inset: schematics of the optical spectra after different optical components.

An experiment based on the setup in Fig. 1 was carried out to demonstrate the proposed method. An optical carrier with power of 10 mW and central wavelength of 1567 nm was applied to be modulated by a microwave signal from an EVNA (HP 8720D) with a frequency sweeping range from 50 MHz to 20 GHz. The optical carrier has a linewidth of 200 kHz and a long-term drift of less than 1 pm. The PM-EOM

(LAAM000) has a bandwidth of 23 GHz with RF and DC half wave voltages of 3.5 V and 16 V, respectively. The driving microwave signal from the EVNA was split into two parts. An electrical hybrid coupler (HC) with a bandwidth of 18 GHz was attached after the EVNA, and it was used to introduce $\pi/2$ phase difference between two parts. The two microwave signals were sent into two ports of the DPMZM1 to obtain carrier suppression OSSB modulation. The DPMZM2 did not carry a drive microwave signal to let the pure optical carrier pass through. An EDFA (JDSU) with the maximum output optical power of 10 mW was used to keep the average optical power constant at the PD input. The OSSB modulated signal was sent into the PD via a polarizer and PC2 to convert from an optical signal to an electrical signal. The PD has a bandwidth of 20 GHz and a responsivity of 0.8 A/W. The ODUT is an FBG of a commercial product. The optical spectra in the experiment were recorded by an optical spectrum analyzer (OSA) with a minimum resolution of 0.01 nm.

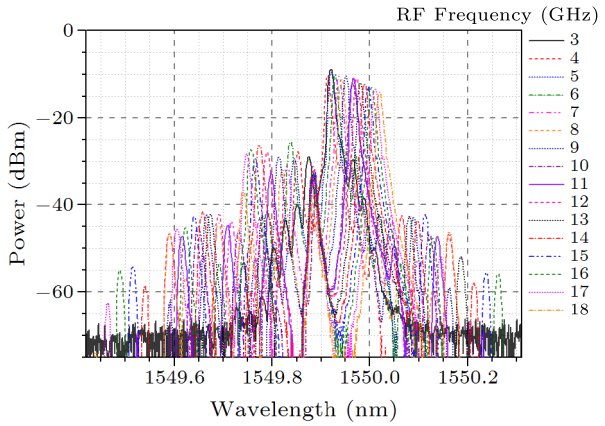

Fig. 2. Measured optical frequency shifting of the OSSB modulation.

First of all, the OSSB modulation was obtained. The bias voltages ($V1$, $V2$, and $V3$) for DPMZM1 were set. Figure 2 shows the measured optical frequency shifting of the OSSB modulations at the output of PM-EOM. The driving microwave signal is of a frequency from 3 GHz to 18 GHz and power of 5 dBm. As can be seen from Fig. 2, the undesired first-order sideband is suppressed by about 25 dB, and the second order sideband is lower than the wanted first-order sideband by about 20 dB to avoid inducing extra measurement errors. The wavelength shifting of the OSSB is about 0.12 nm while the RF frequency is tuned from 3 GHz to 18 GHz. It is worth noting that the OSSB modulation was achieved without an OBPF, which usually introduces optical wavelength dependence. To avoid generating a high-order sideband, the phase modulation index was set to be $\beta = 0.49$. In the first step, we optimized the bias voltages to obtain the largest SSR[9,13] for improving the dynamic range of the OVNA. In the second step, we changed the power ratio (A_0/A_1) by adjusting the bias voltages and kept the total input power constant by tuning the pump power of the EDFA before the PD. Then, the OSSB modulation with a tunable OCSR was achieved. Figure 3 shows the measured optical spectra with tunable OCSR over a ratio change range of 15.9 dB by changing the bias voltages of DPMZMs. The bias voltages of DPMZM1 were set at $V_1 = V_2 = V_{\mathrm{DC}_\pi}$ to totally suppress the optical carrier. The bias voltages of DPMZM1 V_4 and V_5 were tuned to achieve the tunable OCSR. The EDFA was attached after the PM-EOM to control the average input power for the PD to be 1 mW. The maximum input power of the PD is 2 mW. We used an FBG as an ODUT, which has a notch.

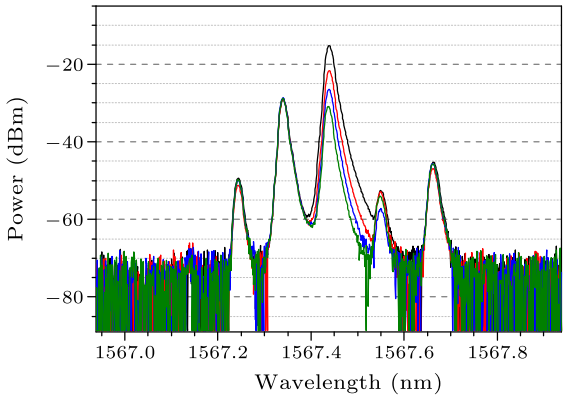

Fig. 3. Measured optical spectra of the OSSB modulation with a tunable OCSR.

The transmission responses of the ODUT were measured by different methods. We made a calibration without the ODUT before measuring its magnitude and phase response. In the first experiment, we set the OCSR to be 13.5 dB to measure both magnitude and phase response of the ODUT as shown in Figs. 4(a) and 4(b) in black lines when the phase modulation index $\beta = 0.49$. The measurement error due to the undesired sidebands can be neglected. We selected the sweeping points of the EVNA to be 1601 over a frequency range of 8 GHz, and hence the corresponding measured resolution is 5 MHz. Therefore, the resolution of the OVNA is 5 MHz, which is smaller than the best commercial OSA or commercial OVNA [LUNA CTe OVA 4000]. The resolution can be further optimized by reducing the measurement frequency range because the EVNA in our lab has the maximum setting point number of 1601. Then, we changed the OCSR into −2.3 dB and tuned the gain of the EDFA for keeping average power identical, and then we performed the same measurement. Figures 4(a) and 4(b) show the measured magnitude and phase responses in red lines. The improvement of dynamic range, considering the magnitude response measurement based on a larger OCSR as reference, is calculated to be

3.7 dB. A zoom in view is given in Fig. 4(a) to show the difference between the two cases. As can be seen from Fig. 4(a), some ripples appear, which are attributed to the interference induced by the undesired sidebands. The measured deviation between the two cases can be attributed to the dynamic range improvement of the proposed OVNA. It is worth noting that noise appears around the center of the FBG and the measured magnitude response can overlap with each other except the frequency from 9.6 GHz to 11.3 GHz. The bandwidth of the proposed system is limited by the working bandwidth of the electrical HC. When the ODUTs are polarization-dependent components, the polarization-dependent loss and polarization mode dispersion should be measured.[17]

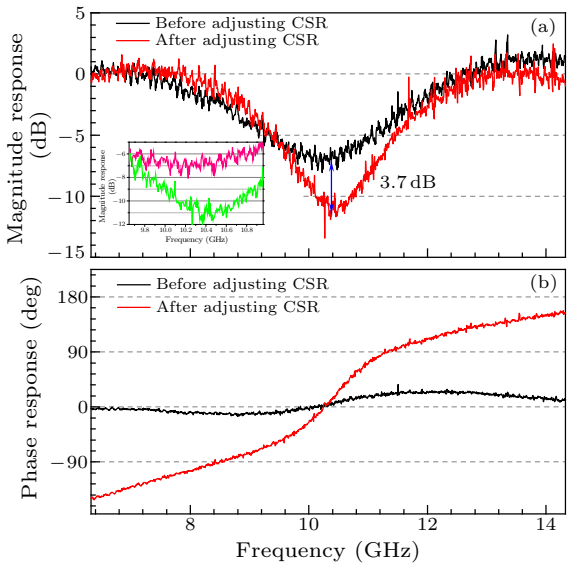

Fig. 4. Measured transmission response of the ODUT using different schemes: (a) magnitude response and (b) phase response.

In summary, we have demonstrated a new and simple approach to achieve an OVNA based on a PM-EOM without an OBPF. The proposed method can effectively improve the dynamic range of the OVNA under small signal modulation avoiding extra measurement errors. The bias voltages of the DPMZM1 are tuned to achieve optical carrier frequency shifting to realize OSSB modulation. The bias voltages of the DPMZM2 are set to achieve a tunable OCSR. We first optimize the SSR to be the largest. By improving the OCSR and keeping the optical power constant at the PD input, we have achieved dynamic range improvement with 3.7 dB for magnitude response. We have theoretically analyzed and experimentally demonstrated the proposed OVNA. The magnitude and phase responses have been obtained by the proposed approach.

References

[1] Loayssa A and Benito D 2004 *Opt. Eng.* **43** 2418
[2] Simova E, Berini P and Grover C P 2001 *J. Lightwave Technol.* **19** 717
[3] VanWiggeren G D, Motamedi A R and Barley D M 2003 *IEEE Photon. Technol. Lett.* **15** 263
[4] Li W, Wang W T, Sun W H et al 2014 *IEEE Photon. J.* **6** 7901108
[5] Xue M, Zhao Y, Gu X et al 2013 *J. Opt. Soc. Am.* B **30** 928
[6] Román J E, Frankel M Y and Esman R D 1998 *Opt. Lett.* **23** 939
[7] Loayssa A, Hernández R, Benito D et al 2004 *Opt. Lett.* **29** 638
[8] Sagues M and Loayssa A 2010 *Opt. Express* **18** 17555
[9] Wang M and Yao J 2013 *IEEE Photon. Technol. Lett.* **25** 753
[10] Xue M, Pan S and Zhao Y 2014 *Opt. Lett.* **39** 3595
[11] Wang W T, Li W, Liu J G et al 2014 *IEEE Photon. J.* **6** 5501310
[12] Li W, Sun W H, Wang W T et al 2014 *IEEE Photon. Technol. Lett.* **26** 866
[13] Xue M, Pan S L and Zhao Y J 2016 *Appl. Phys.* B **122** 1
[14] Shimotsu S, Oikawa S, Saitou T et al 2001 *IEEE Photon. Technol. Lett.* **13** 364
[15] Izutsu M, Shikama S and Sueta T 1981 *IEEE J. Quantum Electron.* **17** 2225
[16] Lim C, Attygalle M, Nirmalathas A et al 2006 *IEEE Trans. Microwave Theory Tech.* **54** 2181
[17] Sagues M, Perez M and Loayssa A 2008 *Opt. Express* **16** 16181